Journal of Organometallic Chemistry, *452* (1993) 105–109

JOM 23396

Novel dimeric structure in the Pd^{II} complex of 1,10-dithia[2](2,6)pyridino[2](1,1′)ferrocenophane. A connected metal–metal interaction

Masaru Sato and Hirofumi Asano
Chemical Analysis Center, Saitama University, Urawa, Saitama 338 (Japan)

Sadatoshi Akabori
Department of Chemistry, Faculty of Science, Toho University, Funabashi, Chiba 274 (Japan)

(Received September 5, 1992; in revised form November 20, 1992)

Abstract

The $Pd(BF_4)_2$ complex of 1,10-dithia[2](2,6)pyridino[2](1,1′)ferrocenophane was prepared. The NMR spectral data suggested that the complex has a weak dative bond between the Pd and Fe atoms. The X-ray analysis of the complex supported the suggestion and also showed that a weak Pd–Pd bonding interaction connects two molecules, resulting in a novel dimeric structure.

1. Introduction

Bonding interaction between the metal atoms in binuclear complexes is an interesting topic in orgnometallic chemistry. That a dative metal–metal bond could participate with the Fe atom of ferrocene was first found in the product (1) of reaction between 1,2,3-trithia[3]ferrocenophane and tetrakis(triphenylphosphine)palladium(0) [1]. The same phenomenon in the Pt^{II} analogue (2) was then reported [2,3]. Trithia[*n*]ferrocenophane (3, 4) [4,5], 1,1-bis(alkylthio)ferrocene (5) [6,7], and 1,1′-bis(diphenylphosphino)ferrocene (6) have all been found to afford the same type of complex. Recently, cluster complexes involving a dative metal–metal bond between the Fe atom of ferrocene and the Ru [8] or Os atom [9] have also been reported. We now report the preparation and a single crystal X-ray analysis of the $Pd(BF_4)_2$ complex of 1,10-dithia[2](2,6)pyridino[2](1,1′)ferrocenophane.

2. Results and discussion

1,10-Dithia[2](2,6)pyridino[2](1,1′)ferrocenophane (7), which was prepared from disodium 1,1′-ferrocenedithiolate and 2,6-bis(bromomethyl)pyridine [10], reacted with $(MeCN)_4Pd(BF_4)_2$ in acetonitrile to give (acetonitrile) {1,10-dithia[2](2,6)pyridino[2](1,1′)ferrocenophane-S,S,Fe}palladium(II) tetrafluoroborate (8) as dark green crystals in good yield. In the ^1H NMR spectrum of 8, the bridging methylene protons appeared as an AB pattern ($J = 18$ Hz) at δ 4.56 and 5.12, unlike the singlet (δ 4.16) in the free ligand, suggesting that the complex has a rigid conformation. The ring protons of pyridine resonated at lower field (δ 7.51 and 8.05) than those of the free ligand (δ 7.08 and 7.56). Coordination of the nitrogen atom of pyridine to

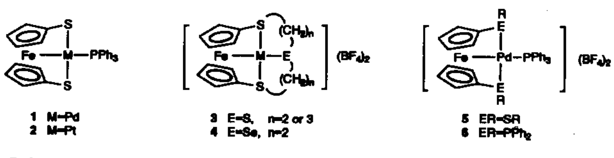

Scheme 1.

Correspondence to: Dr. M. Sato.

0022-328X/93/$6.00

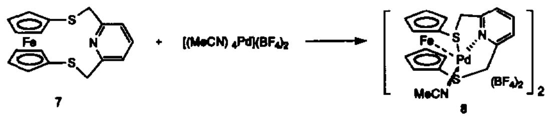

Scheme 2.

the Pd^{II} atom seems to be responsible for this low-field shift of the ring protons of pyridine. Two multiplets at δ 5.02 and 5.19 and two multiplets at δ 3.40 and 4.13 were assigned as the β- and α-protons of the ferrocene ring by 2D H,H-COSY experiments, respectively. These shifts, observed on complexation, to lower-field of the β-protons and to higher-field shift of the α-protons of the ferrocenyl ring when compared with those of the free ligand, are considered as evidence for a dative bond between the Fe atom of ferrocene and the Pd^{II} atom [4–7]. This is because the β- and α-protons of the ferrocene ring were observed at δ 4.42 and 5.28, respectively, in the $PdCl_2$ complex of 1,1'-bis(isobutylthio)ferrocene in which there is no interaction between the Fe and Pd atoms [11]. The C–H out-of-bending vibration of the ferrocene ring, which is a diagnostic probe for the oxidation state of ferrocene [12], is observed at 824 cm^{-1} in complex **8**. This is in a higher-frequency region than that of the free ligand **7** (806 cm^{-1}), but in a considerably lower-frequency region than that of complex **4** (844 cm^{-1}) [5]. This seems to imply that the dative bond between the Fe and Pt atoms in this complex is much weaker than in complex **4**. The cyclic voltammogram of complex **8** was measured in 0.1 M $[(C_4H_9)_4N]ClO_4$/acetonitrile at room temperature. One irreversible wave ($E_{pc} = -0.49$ V) and one reversible wave ($E_{pc} = +0.61$ and $E_{pa} = +0.68$ V) were observed. The former was assigned as a Pd^I/Pd^{II} redox couple and the latter as an Fe^{II}/Fe^{III} couple, by reference to the related complexes $Fe(C_5H_4SR)_2PdCl_2$ [13]. The corresponding potential for complex **5** (R = ^{i}Bu), which has a dative Fe–Pd bond [7], is $E_{pc} = -0.58$ and $E_{pa} = 0.98$ V. The Pd and Fe couples for complex **8** are shifted to a low-potential region by 0.11 and 0.30 V respectively, compared with those for complex **5**. The Fe couple for complex **5** in the high-potential region seems to appear because the electron density on the Fe atom in complex **5** is decreased by an Fe–Pd dative bond. Therefore, the result may suggest that there is only a little, if any, bonding interaction between the Fe and Pd atoms in complex **8**.

The molecular structure of **8** was determined by single crystal X-ray diffraction and is shown in Fig. 1. The bond distances and bond angles in **8** are summarized in Tables 1 and 2. The molecule consists of two symmetrically related complexes with a Pd–Pd interaction, two BF_4 anions and one molecule of acetonitrile being present in the outer sphere. In each part of the molecule, the coordination sphere around the Pd atom is a slightly distorted square-planar with two S atoms and two N atoms in *trans* positions (Pd–S 2.280, 2.320(4) Å, Pd–N 1.91, 2.00(1) Å). These Pd–S distances are almost the same as those in the Pd^{II} quasi-octahedral complex of 1,4,10,13-tetrathia-7,16-diazacyclooctadecane (Pd–S, 2.311 and 2.357 Å) [14], while the Pd–N distances are near the lower limit for those in most Pd complexes (2.0–2.2 Å) [15]. The

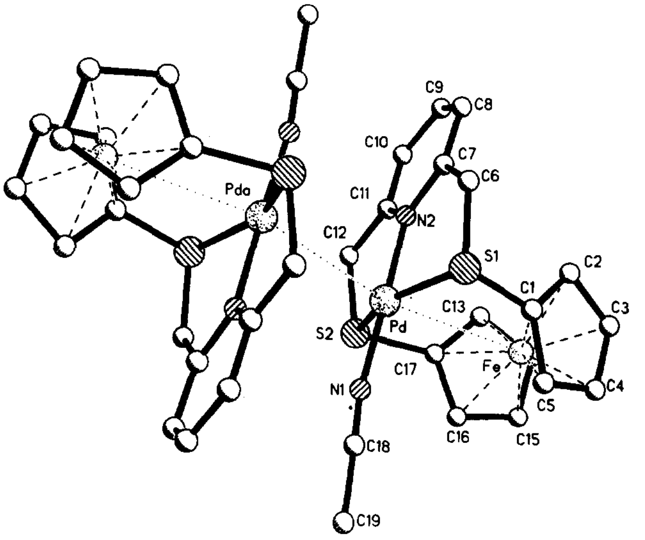

Fig. 1. Molecular structure of complex **8**.

TABLE 1. Bond distances (Å) for complex **8**

Pd–Pd	3.278(2)	Pd–Fe	3.228(2)
Pd–S(1)	2.280(4)	Pd–S(2)	2.320(4)
Pd–N(1)	2.00(1)	Pd–N(2)	1.91(1)
Fe–C(1)	2.10(2)	Fe–C(2)	2.07(2)
Fe–C(3)	1.95(2)	Fe–C(4)	1.96(2)
Fe–C(5)	2.08(2)	Fe–C(13)	2.04(2)
Fe–C(14)	2.01(2)	Fe–C(15)	1.96(2)
Fe–C(16)	2.09(2)	Fe–C(17)	2.06(2)
S(1)–C(1)	1.77(2)	S(1)–C(6)	1.79(2)
S(2)–C(12)	1.76(2)	S(2)–C(17)	1.80(2)
N(1)–C(18)	1.13(3)	N(2)–C(7)	1.38(2)
N(2)–C(11)	1.37(2)	C(1)–C(2)	1.39(2)
C(1)–C(5)	1.41(2)	C(2)–C(3)	1.37(2)
C(3)–C(4)	1.38(2)	C(4)–C(5)	1.37(2)
C(6)–C(7)	1.52(2)	C(7)–C(8)	1.35(2)
C(8)–C(9)	1.36(2)	C(9)–C(10)	1.35(2)
C(10)–C(11)	1.37(2)	C(11)–C(12)	1.40(2)
C(13)–C(14)	1.37(2)	C(13)–C(17)	1.39(2)
C(14)–C(15)	1.38(2)	C(15)–C(16)	1.40(2)
C(16)–C(17)	1.37(2)	C(18)–C(19)	1.47(3)
B(1)–F(1)	1.35(2)	B(1)–F(2)	1.35(2)
B(1)–F(3)	1.32(2)	B(1)–F(4)	1.34(2)
B(2)–F(5)	1.33(2)	B(2)–F(6)	1.38(2)
B(2)–F(7)	1.31(2)	B(2)–F(8)	1.36(2)
N(3)–C(20)	1.19(3)	C(20)–C(21)	1.32(4)

square is slightly distorted by bending along the N(1)–N(2) plane so that the S–Pd–S angle decreases to 153.3(2)°. The coordination structure of the Pd atom is completed as quasi-octahedral by weak bonds with the Fe atom and with another Pd atom (Pd–Fe 3.228(2) Å, Pd–Pd 3.278(2) Å, Fe–Pd–Pd 166.48(6)°). A quasi-octahedral stereo-chemistry around the Pd^{II} atom with a significant apical interaction is also reported in the Pd^{II} complexes of 1,4,7-trithiacyclononane [16], 1,4,7,10,13,16-hexathiacyclooctadecane [17], and 1,4,10,13-tetrathia-7,16-diazacyclooctadecane [14], but apical interaction with other transition metals is rare in the square-planar Pd^{II} complexes.

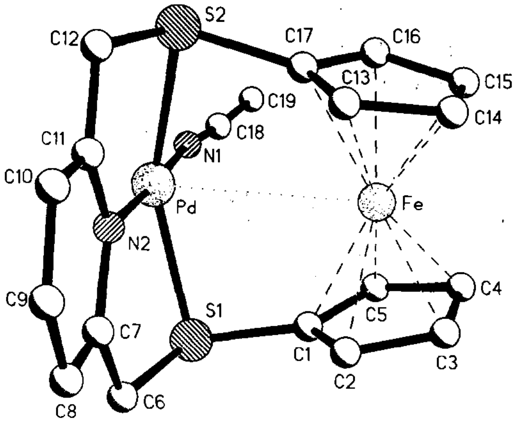

Fig. 2. Side view of one of a pair of **8**.

The side view for one of a pair of **8** is shown in Fig. 2. Both Cp rings of the ferrocene moiety in **8** are practically planar since the maximal deviation of the C atoms from the mean plane is only 0.05 Å. They are not parallel and the tilting angle between mean planes of Cp rings is 17.8°. The Fe–Pd distance (3.228(2) Å) in **8** is fairly long compared with dative Fe–Pd bond distances reported in (triphenylphosphine) (ferrocene-1,1′-dithiolato-S,S,Fe)-palladium(II) (**1**) (2.878 Å) [1] and (1,9-dithia-5-selena[9]ferrocenophane-S,S,Se, Fe)palladium(II) tetrafluoroborate (**4**) (3.028(2) Å) [18], while the distance between Fe and Pd in dichloro{1,1′-bis(isobutylthio)-ferrocene-S,S}palladium(II) is 3.810 Å [11]. However, the tilting angle between mean planes of Cp rings (17.8°) and the angle S–Pd–S (153.3(2)°) are similar to those in **1** (19.6 and 168.6°) and **4** (19.2 and 156.9°), while the corresponding angles in dichloro{1,1′-bis(isobutylthio)ferrocene-S,S}palladium are 1.9 and 83.9° respectively. This fact suggests the presence of a weak Fe–Pd dative bond. Elongation of the Fe–Pd distance may be due to avoidance of conformational strain imposed by adoption of a square-planar arrangement around the Pd^{II} atom by the dithiaazaferrocenophane and acetonitrile. The Pd–Pd distance (3.278(2) Å) in **8** seems to indicate no direct bonding, because the Pd–Pd single bond length lies in the range 2.531–2.699 Å [15b]. However, a weak bonding interaction may be required in order to hold a quasi-octahedral configuration around the Pd^{II} atom in **8**, resulting in a strange dimeric structure and a connected metal–metal interaction, Fe–Pd–Pd–Fe. To the best of our knowledge, such interaction involving metallocene is unprecedented, although some consecutive metal-sequences containing other metals are known [19–21].

TABLE 2. Selected bond angles (°) for complex **8**

Pd–Pd–Fe	166.48	Pd–Pd–S(1)	91.0(1)
Pd–Pd–S(2)	113.8(1)	Pd–Pd–N(1)	90.3(4)
Pd–Pd–N(2)	87.3(4)	Fe–Pd–S(1)	76.9(1)
Fe–Pd–S(2)	77.3(1)	Fe–Pd–N(1)	96.6(4)
Fe–Pd–N(2)	85.9(4)	S(1)–Pd–S(2)	153.3(2)
S(1)–Pd–N(1)	94.9(4)	S(1)–Pd–N(2)	86.3(4)
S(2)–Pd–N(1)	94.7(4)	S(2)–Pd–N(2)	85.3(4)
N(1)–Pd–N(2)	177.4(5)	Pd–S(1)–C(1)	91.3(5)
Pd–S(1)–C(6)	95.4(6)	C(1)–S(1)–C(6)	104.1(8)
Pd–S(2)–C(12)	94.0(7)	Pd–S(2)–C(17)	88.3(6)
C(12)–S(2)–C(17)	105.0(9)	Pd–N(1)–C(18)	168(1)
Pd–N(2)–C(7)	126(1)	Pd–N(2)–C(11)	121(1)
C(7)–N(2)–C(11)	113(1)	Fe–C(1)–S(1)	129.5(9)
S(1)–C(1)–C(2)	125(1)	S(1)–C(1)–C(5)	121(1)
C(2)–C(1)–C(5)	114(1)	C(1)–C(2)–C(3)	98(1)
C(2)–C(3)–C(4)	117(2)	C(3)–C(4)–C(5)	104(1)
C(1)–C(5)–C(4)	106(1)	S(1)–C(6)–C(7)	117(1)
N(2)–C(7)–C(6)	110(1)	N(2)–C(7)–C(8)	130(2)
C(6)–C(7)–C(8)	120(1)	C(7)–C(8)–C(9)	113(2)
C(8)–C(9)–C(10)	123(2)	C(9)–C(10)–C(11)	120(2)
N(2)–C(11)–C(10)	121(1)	N(2)–C(11)–C(12)	116(2)
C(10)–C(11)–C(12)	123(2)	S(2)–C(12)–C(11)	117(1)
C(14)–C(13)–C(17)	108(1)	C(13)–C(14)–C(15)	105(1)
C(14)–C(15)–C(16)	112(1)	C(15)–C(16)–C(17)	103(1)
Fe–C(17)–S(2)	132.5(9)	S(2)–C(17)–C(13)	129(1)
S(2)–C(17)–C(16)	120(1)	C(13)–C(17)–C(16)	111(1)
N(1)–C(18)–C(19)	176(2)		

3. Experimental section

The IR spectra were taken on a Hitachi 270-50 infrared spectrometer. The ^1H and ^{13}C NMR spectra were measured on a Bruker AM 400 Spectrometer.

3.1. Materials

1,10-Dithia[2](2,6)pyridino[2](1,1′)ferrocenophane (**7**) [10] and dichlorobis(acetonitrile)palladium(II) [22] were prepared according to methods described in the literature.

3.2. (Acetonitrile){1,10-dithia[2](2,6)pyridino[2](1,1′)-ferrocenophane-S,S,Fe}palladium tetrafluoroborate (8)

A mixture of $(CH_3CN)_2PdCl$ (27 mg, 0.1 mmol) and $AgBF_4$ (42 mg, 2.2 mmol) in dry CH_3CN (4 ml) was refluxed for 1 h. To the mixture compound **7** (36 mg, 1 mmol) in benzene (4 ml) and CH_3CN (4 ml) was added. After several minutes the mixture was filtered. The filtrate was evaporated under vacuum. The residue was dissolved in CH_3CN (1 ml) and acetone (1 ml) and the solution filtered. To the filtrate dry ether (2 ml) was added and the solution was kept overnight in a freezer. Dark green needles were precipitated and collected by filtration (50 mg, 79%). M.p. > 250°C. Found: C, 34.57; H, 2.82; N, 5.03; $C_{17}H_{15}B_2F_8NS_2$-$FePd \cdot 3/2CH_3CN$ calcd.: C, 34.28; H, 2.99; N, 5.01%. IR (KBr): 3072, 2908, 1596, 1466, 1300, 1074, 1036, 880, and 824 cm^{-1}. ^1H NMR (CD_3CN) δ 3.39 (m, 2H, H_α), 4.13 (m, 2H, H_α), 4.56 (d, $J = 18$ Hz, CH_2), 5.02 (m, 2H, H_β), 5.12 (d, $J = 18$ Hz, CH_2), 5.19 (m, 2H, H_β), 7.51 (d, 2H, $J = 8$ Hz, $H_{3,5}$ in Py), and 8.05 (t, $J = 8$ Hz, H_4 in Py). ^{13}C NMR (CD_3CN) δ 45.02 (CH_2), 67.81 (C_α), 70.69 (C_α), 75.68 (C_β), 77.28 (C_{ipso}), 77.69 (C_β), 125.03 ($C_{3,5}$ in Py), 143.43 (C_4 in Py), 159.54 ($C_{3,5}$ in Py).

TABLE 3. Atomic coordinates and isotropic and equivalent isotropic thermal parameters. $U_{eq} = 1/3\ \Sigma_i \Sigma_j\ U_{ij} a_i a_j a_i^* a_j^*$

Atom	x	y	z	U_{iso} / U_{eq}
Pd	0.4558(1)	0.0852(1)	0.0631(1)	0.028(1)
Fe	0.4013(2)	0.3123(2)	0.1764(1)	0.034(3)
S(1)	0.4808(3)	0.2971(4)	0.0120(2)	0.037(5)
S(2)	0.4317(4)	−0.0567(4)	0.1564(2)	0.040(5)
N(1)	0.321(1)	0.060(1)	0.0195(6)	0.031(9)
N(2)	0.587(1)	0.102(1)	0.1027(6)	0.04(1)
C(1)	0.442(1)	0.390(2)	0.0829(8)	0.05(1)
C(2)	0.503(1)	0.443(2)	0.1370(7)	0.06(1)
C(3)	0.434(1)	0.513(2)	0.1707(9)	0.04(1)
C(4)	0.338(1)	0.492(2)	0.1485(8)	0.07(1)
C(5)	0.342(1)	0.416(2)	0.0893(8)	0.05(1)
C(6)	0.611(1)	0.293(2)	0.0269(8)	0.06(1)
C(7)	0.654(1)	0.202(2)	0.0857(8)	0.06(1)
C(8)	0.745(1)	0.226(2)	0.1126(8)	0.05(1)
C(9)	0.772(1)	0.139(2)	0.1664(8)	0.04(1)
C(10)	0.714(1)	0.034(2)	0.1865(8)	0.05(1)
C(11)	0.621(1)	0.018(2)	0.1565(8)	0.07(1)
C(12)	0.557(1)	−0.088(2)	0.1750(8)	0.04(1)
C(13)	0.468(1)	0.180(2)	0.2473(8)	0.06(1)
C(14)	0.414(1)	0.280(2)	0.2778(8)	0.05(1)
C(15)	0.320(1)	0.261(2)	0.2497(8)	0.04(1)
C(16)	0.312(1)	0.147(2)	0.2042(8)	0.07(1)
C(17)	0.406(1)	0.101(2)	0.2029(8)	0.05(1)
C(18)	0.240(2)	0.062(2)	0.0028(8)	0.04(1)
C(19)	0.136(1)	0.055(2)	−0.0197(8)	0.07(2)
B(1)	0.047(1)	0.226(2)	0.1337(9)	0.08(1)
B(2)	0.769(1)	0.637(2)	0.1223(9)	0.10(1)
F(1)	0.0714(8)	0.088(1)	0.1428(5)	0.12(1)
F(2)	0.1264(8)	0.279(1)	0.1066(6)	0.14(1)
F(3)	−0.0276(8)	0.253(1)	0.0888(6)	0.11(1)
F(4)	0.0328(8)	0.270(1)	0.1970(5)	0.10(1)
F(5)	0.7722(8)	0.595(1)	0.0582(5)	0.11(1)
F(6)	0.8163(7)	0.528(1)	0.1573(5)	0.13(1)
F(7)	0.6928(8)	0.627(1)	0.1584(6)	0.12(1)
F(8)	0.8276(8)	0.741(1)	0.1503(5)	0.10(1)
N(3)	0.214(1)	0.766(1)	0.0713(6)	0.07(1)
C(20)	0.143(2)	0.694(2)	0.061(1)	0.07(1)
C(21)	0.064(2)	0.614(2)	0.052(1)	0.10(2)
H(2A)	0.576	0.437	0.145	
H(3A)	0.452	0.566	0.214	
H(4A)	0.278	0.527	0.169	
H(5A)	0.286	0.384	0.058	
H(6A)	0.632	0.393	0.035	
H(6B)	0.638	0.262	−0.016	
H(8A)	0.791	0.295	0.094	
H(9A)	0.835	0.155	0.194	
H(10A)	0.740	−0.034	0.223	
H(12A)	0.576	−0.178	0.154	
H(12B)	0.568	−0.100	0.226	
H(13A)	0.541	0.167	0.256	
H(14A)	0.438	0.353	0.312	
H(15A)	0.263	0.318	0.263	
H(16A)	0.252	0.112	0.176	

3.3. Structure determination

Crystal data of **8**: $C_{21}H_{21}B_2F_8FeN_3PdS_2$, M = 715.4, monoclinic, space group $P2_1/n$, $a = 13.750(5)$, $b = 9.447(4)$, $c = 19.688(7)$ Å, $\beta = 94.78(3)°$, $V = 2549(2)$ Å^3, $Z = 4$, $D_x = 1.865$ g cm^{-1}, μ(Mo Kα) = 15.0 cm^{-1}, $F(000) = 1416$, $T = 295$ K, crystal size 0.15 × 0.18 × 0.32 mm.

Data collection was performed at room temperature on an Enraf-Nonius CAD-4 diffractometer using graphite-monochromated Mo Kα radiation (λ = 0.71069 Å) in ω scan technique (2θ max 54°). Cell parameters were determined from a least-squares fitting of 24 reflections, $22 < 2\theta < 26°$. Crystal and instrument stability were monitored by measurement of two check reflections every 2 h: 0 2 −10 and 1 5 2. From 5214 reflections measured, 1518 independent reflections with $I > 2\sigma(I)$ were used for refinement. The Ψ-scan method was applied to absorption correction.

Positions of Pd and Fe atoms were revealed by the Patterson method and positions of other non-H atoms were determined in three subsequent difference maps. The H atoms were positioned according to the idealized geometry with d(C–H) = 1.00 Å and isotropic $U = 0.06$ Å^2. Pd, Fe, and two S atoms were refined anisotropically and other non-H atoms were refined isotropically using least-squares method with a total of 173 variables; $R = 0.062$ (with unit weight), $S = 2.21$. H atoms in NCMe were not located. Final positional parameters for non-H atoms are listed in Table 3.

References

1 D. Seyferth, B. M. Hames, T. G. Rucker, M. Cowie and R. S. Dickson, *Organometallics, 2* (1983) 472.

2 S. Akabori, T. Kumagai, T. Shirashige, S. Sato, K. Kawazoe, C. Tamura and M. Sato, *Organometallics, 6* (1987) 526.

3 S. Akabori, T. Kumagai, T. Shirashige, S. Sato, K. Kawazoe, C. Tamura and M. Sato, *Organometallics, 6* (1987) 2105.
4 M. Sato, K. Suzuki and S. Akabori, *Chem. Lett.*, 1987, 2239.
5 M. Sato, H. Asano, K. Suzuki, M. Katada and S. Akabori, *Bull. Chem. Soc. Jpn., 62* (1989) 3828.
6 M. Sato, M. Sekino and S. Akabori, *J. Organomet. Chem., 344* (1988) C31.
7 M. Sato, M. Sekino, M. Katada and S. Akabori, *J. Organomet. Chem., 377* (1989) 327.
8 M. I. Bruce, P. A. Humphrey, O. B. Shawkataly, M. R. Snow, E. R. T. Tiekink and W. R. Cullen, *Organometallics, 9* (1990) 2910.
9 W. R. Cullen, S. J. Rettig and T.-C. Zheng, *Organometallics, 11* (1992) 277.
10 M. Sato, S. Tanaka, S. Ebine, K. Morinaga and S. Akabori, *J. Organomet. Chem., 289* (1985) 91.
11 B. McCulloch, D. L. Ward, J. D. Woolins and C. H. Brubacker, Jr., *Organometallics, 4* (1985) 1425.
12 J. A. Kramer and D. N. Hendricson, *Inorg. Chem., 19* (1980) 3330.
13 B. McCulloch, D. L. Ward, J. D. Woolins and C. H. Brubaker, Jr., *Organometallics, 4* (1985) 1425.
14 G. Reid, A. J. Blake, T. I. Hyde and M. Schröder, *J. Chem. Soc., Chem. Commun.*, (1988) 1397.
15 P. M. Maitlis, P. Espinet and M. J. H. Russell, in G. Wilkinson, F. G. A. Stone and E. W. Abel (Eds.), *Comprehensive Organometallic Chemistry*, Pergamon Press, 1982, Vol. 6, pp. 233 and 265.
16 K. Wieghardt, H.-J. Küppers, W. Raabe and C. Krüger, *Angew. Chem. Int. Ed. Engl., 25* (1986) 1101.
17 A. J. Blake, R. O. Gould, A. J. Lavery and M. Schröder, *Angew. Chem. Int. Ed. Engl., 25* (1986) 274.
18 Y. Yokomori and Y. Ohashi, *39th Symp. Coord. Chem. (Japan)*, 1989, p. 769.
19 R. J. Haines, N. D. C. T. Steen and R. B. English, *J. Chem. Soc., Chem. Commun.*, (1981) 587.
20 D. A. Bohling, T. P. Gill and K. R. Mann, *Inorg. Chem., 20* (1981) 194.
21 B. Lippert and D. Neugebauer, *Inorg. Chem., 21* (1982) 451.
22 F. R. Hartley, S. G. Murray and C. A. McAuliffe, *Inorg. Chem., 18* (1979) 1394.